Indian J. Phys. **72B** (5), 515-526 (1998)

IJP B
— an international journal

Diagnostic study of N_2 laser produced plasma on indium target

Smita Tulapurkar, A G Bidve, S S Patil and Sharada Itagi

Department of Physics, Dr Babasaheb Ambedkar Marathwada University, Aurangabad 431004, Maharashtra, India

Received 11 November 1997, accepted 20 July 1998

Abstract Spatially and temporally resolved measurements of spectral lines are carried out to get information about plasma evolution, temperature and density Plasma produced on Indium target by nanosecond pulses of N_2 laser is reported Different models of plasma propagation are tested for the experimental data Electron density in the plasma is estimated from stark width measurement. Time of flight distribution is measured The distribution is full Maxwellian with a centre of mass velocity The temperature thus determined is rather high

Keywords : Plasma evolution, N_2 laser, indium target

PACS Nos. 52 50 Jm, 52 70 Kz

1. Introduction

Understanding of behaviour of material expanding into an ambient gas at low pressure or in vacuum has applications in many fields such as gas dynamics, chemical physics and thin film deposition. When laser pulse deposits energy on a solid target, material is thrown out as plasma plume with large kinetic energy. Processes involved in the laser target interaction and plasma dynamics depend on the properties of both the laser radiation and target material as well as on the surrounding ambient gas. Characteristics of the laser which influence the plasma are fluence, pulse width, and wavelength. Emission spectroscopic studies of the spatial and temporal evolution of the luminous plume gives information about the kinetic energy, ion and electron density and electron temperature of the plasma.

N_2 laser has been used for spectrochemical analysis of solids [1-3]. There are very few investigations on the plasma itself [4-7]. In the present paper, spectral investigation of plasma produced on Indium target using a locally built N_2 laser is reported. Ultraviolet lasers of ns pulse widths and powers of the order of 10^7 W\cm^2 are known to be ideally suitable for thin film deposition [8].

2. Experimental setup

A scheme of experimental setup is shown in Figure 1. Home built N_2 laser ($\lambda = 337.1$ nm) having a pulse duration of 7 ns, repetition rate of 10 Hz and 10^7 W\cm^2 power was used as source. The sample was mounted on a rod and slowly rotated at one end of a vacuum tight metal chamber (15 cm × 5 cm × 5 cm). At the other end of the chamber, a spherical quartz lens (f = 10 cm) is fixed to focus the laser on the target. The laser produced plasma was viewed at right angle to the laser beam through silica windows fixed to the chamber. Using a camera lens plasma plume was imaged (1 : 1 image) on the slit of a monochromator (Carl Zeiss SPM2). For ultraviolet region, a front surface aluminized concave mirror was used. The electrical signal from a cooled photomultiplier (EMI 9816 QB) coupled to the monochromator was fed either to storage oscilloscope (Tektronix 1 466) or boxcar integrator (PAR 162 with 164 integrators). Part of the N_2 laser output was reflected on the surface of a fast photo diode (HP 5880.4220) which supplied trigger to the oscilloscope and signal averager. It was also used to monitor the laser output. The plasma cell and the camera lens and the curved mirror were mounted on a translation stage which allows different regions above the target to be imaged on to the slit of the monochromator A flat smooth surface of Indium sample is obtained by polishing. It is then cleaned with water, dried and fixed at the focus of the quartz lens in the chamber. The chamber is evacuated with a backing pump and filled with air, A or He. Pressure in the chamber is measured with a thermocouple gauge. To avoid pitting the target was rotated continuously.

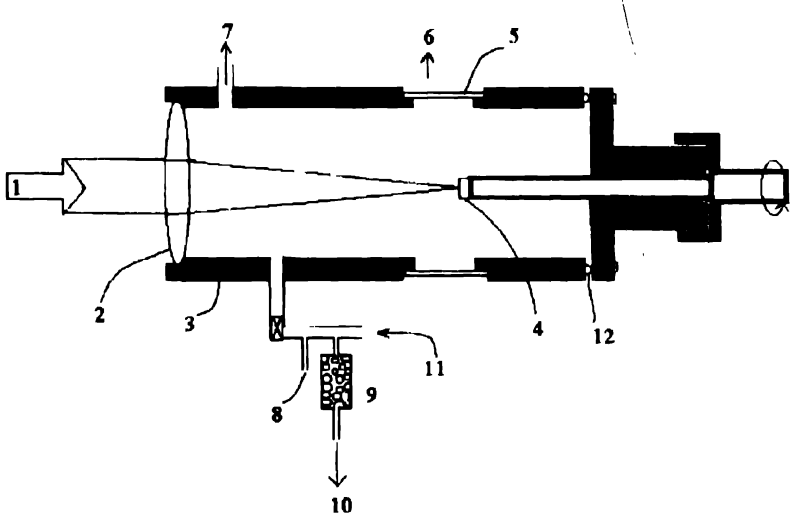

Figure 1. Experimental set up (1) N_2 laser, (2) quartz lens, (3) plasma chamber, (4) target, (5) silica window, (6) monochromator, (7) vacuum gauge, (8) manometer, (9) molecular sieve, (10) rotary pump, (11) gas inlet and (12) 'O' rings

To study the time and space evolution of plasma, a thin slice of the plasma parallel to the target surface is focused on the monochromator slit. For velocity measurement, the distance of the slice from the target is changed and the time of arrival of the pulse is recorded by averaging 20 pulses. For time of flight (TOF) distribution measurement at a distance of 0.5 mm from the target, the time evolution of the pulse is recorded. The monochromator is adjusted at the spectral line center. Aperture duration of the signal averager is kept at 5ns and the aperture delay is scanned upto 150 ns. The plume lasts for less than 85 ns. The measurements are carried

out at 100m Torr air pressure. For line width measurement for a fixed position from the target and a fixed aperture delay the monochromator is scanned to about 10 Å on either side of the spectral line center.

3. Observations and results

The plume produced on Indium target by N_2 laser pulse at low ambient gas pressure has two parts. Very near to the target it is bright and white whereas away from the target it is diffuse blue in colour. In the initial part of the plasma upto about 70 ns or nearly 1.5 mm, spread is one dimensional in the forward direction and then lateral. Indium has large number of lines in blue and violet region. Line at 4104.7 Å, which has no overlap by adjacent lines and which is persistent throughout the plasma, is used to monitor the plasma plume intensity and propagation.

Intensity of the line increases as the distance from the target increases, goes to maximum at 1.5 mm and drops. Figure 2.

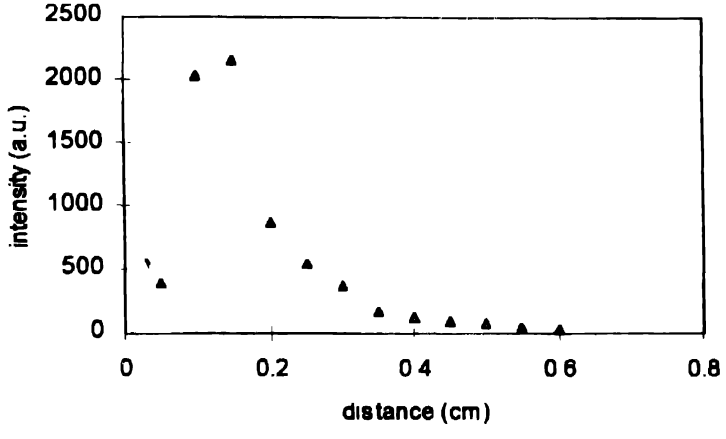

Figure 2. Spatial variation of intensity of 410 47 nm

3.1 Velocity measurement :

At different distances from the target since the pulse lasts for different time intervals the time of arrival of the leading edge of the pulse is recorded. Propagation of leading edge of 4104.7 Å line is measured for 0.1 and 1 Torr air, 1 Torr Ar and He They are shown in Figure 3. Propagation of plasma plume at different ambient gas pressures is described by different models. At low pressures of ambient gas, Geohegan [9] has proposed the drag model. If the mass of ejected material is large, it acts like a piston in a viscous medium. The viscous force is proportional to the velocity of the ablated mass through the background gas. The relation between the distance d from the target and time of arrival t is given by [10]

$$d = \frac{v_p}{c}\left[1 - \exp(-ct)\right] - d_0, \tag{1}$$

where V_p is the initial velocity, c is the slowing coefficient. d_0 is the correction is distance d. d_0 is required to account for the delay in emission of the plasma after the incidence of the laser

radiation on the target surface [10]. In the initial stages of plasma propagation, since the mass of ablated material is large compared to the mass it displaces, the drag model holds good. As the ambient gas is compressed by the ejecta and the ejecta expands farther away from the

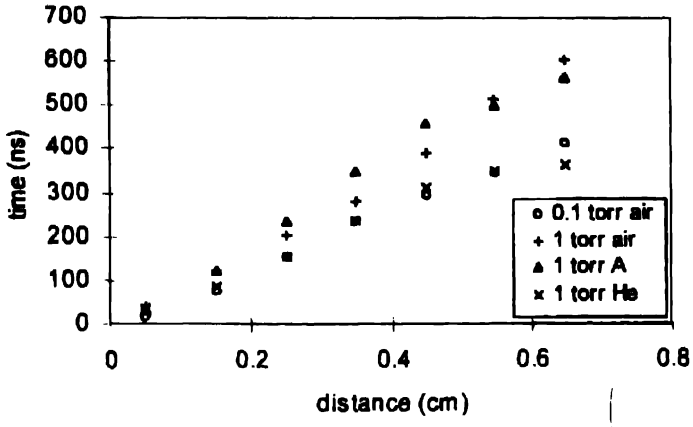

Figure 3. Time evolution in different gases

target, shock model is expected to hold good. For spherical shock wave, distance time relationship is d = constant.$t^{0.4}$ and for plane shockwave, d = constant.$t^{0.6}$ [11]. In the present work a general expression is tried.

$$d = x.\ t^{n} \tag{2}$$

where x and n are varied to fit the experimental data. In Figure 4, the fit of drag model and equation (2) are given. Excellent agreement is seen between drag model and experimental

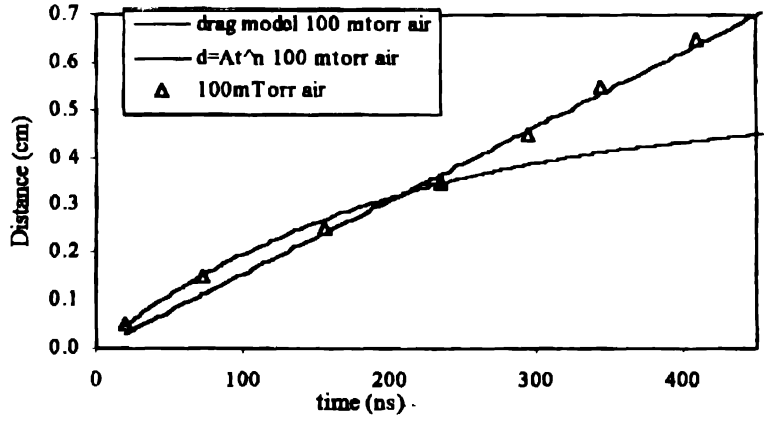

Figure 4. Model fitting of time evolution data at 100 mtorr air.

values upto 2 mm and equation (2) beyond 2 mm as seen in Figures (4-7). The best fit values for different ambient gases are given in Table 1.

Table 1. The best fit values of propagation model

Ambient gas	X	n	V_p/C cm	Slowing coeffi C 1/s	d_o (cm)
100 mtorr air	1.55×10^6	1.0	5.15	400000	0
1 torr air	60000	0.8	1.95	650000	−0.005
1 torr Ar	2955	0.6	2	650000	0
1 torr helium	275000	0.89	4.9	390000	0.015

3.2 Temperature measurements :

Boltzmann plot method is a simple common method of determining excitation temperature from emission data. It assumes that the intensity of an emission line is directly proportional to the

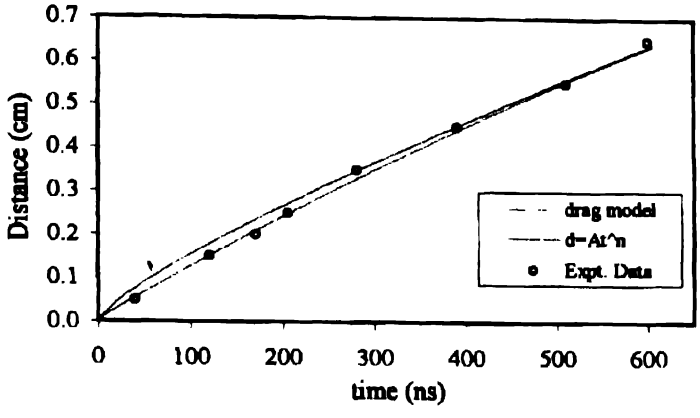

Figure 5. Model fitting of time evolution data at 1 Torr air

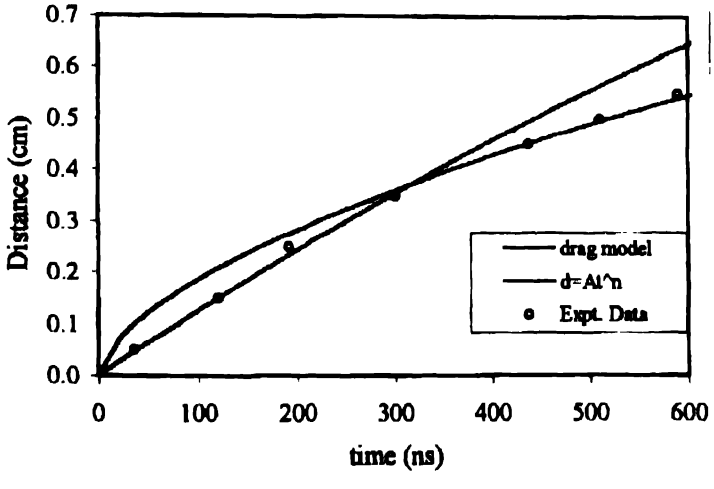

Figure 6. Model fitting of time evolution at 1 Torr Argon

number of atoms in the excited upper state. Excitation temperature determines the number in different excited states, if plasma is in local thermodynamic equilibrium. Boltzmann equation is

$$I \alpha (gf / \lambda^3) \exp(-E / kT), \tag{3}$$

where λ, f, I are wavelength, oscillator strength and intensity of the line and E, g are respectively excitation energy and statistical weight of the upper state and k is Boltzmann constant in cm^{-1}

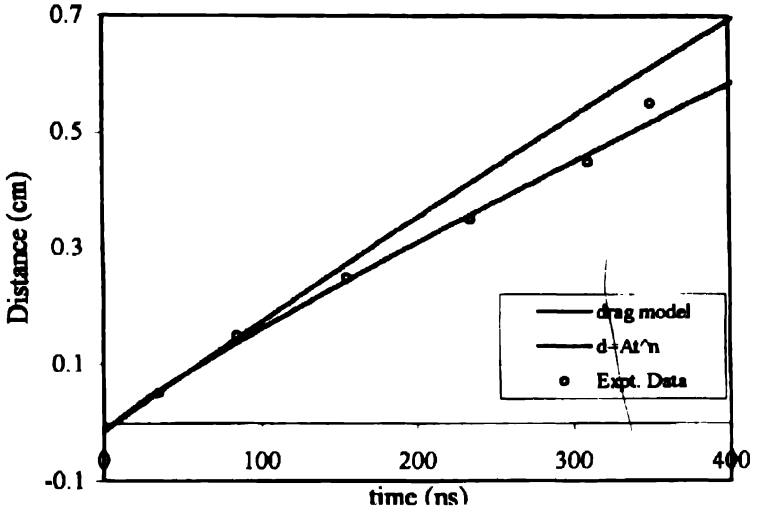

Figure 7. Model fitting of time evolution at 1 Torr Helium

To determine the excitation temperature, intensities of lines with well spread upper energy levels have to be measured. In the present experiment, for lines 2521.3 Å, 2601.7 Å, 2710.2 Å, intensities have been measured at four different distances from the target. Statistical weight, transition probabilities and energy heights have been taken from [12]. Plot of E against [-ln ($I\lambda^3$ /gf)] for three spectral lines at four different distances are shown in Figure 8. Slopes of these straight lines give 1/kT. Temperatures determined are 11400 K, 4600 K, 4300 K, 3500 K at 0.5 mm, 1.5 mm, 2.5 mm, and 3.5 mm from the target respectively. Temperature is maximum near the target and then it drops.

3.3 Time of flight distribution :

The time of flight measurements give an excellent technique to determine the velocity distribution of any species in the plasma. When large amount of energy is deposited in a single pulse of laser, the laser solid interaction gives kinetic energy to the ejecta. The ejected products move with great velocity. The shape of the velocity distribution depends on the temperature of the ejecting solid as well as interactions after the ejection. For thermal emission with low number densities, the velocity distribution is half Maxwellian. The velocities normal to the target take only positive values. At higher number densities because of collisions among the ejected particles within a thin layer known as Knudsen layer (KL), the velocity distribution function is full range Maxwellian (MB) in the centre of mass coordinate (C.O.M.) system [13].

$$\text{signal} = A.d.t^{-4} \exp\left| -\beta^2 \frac{(d - V_0 t)^2}{,^2} \right. \tag{4}$$

The peak velocity V' deduced from the maximum of TOF distribution is related to centre of mass velocity V_0 and temperature T through

$$V' = \frac{V_0}{2} + \sqrt{\frac{V_0^2}{4} + \frac{4kT}{m}} \tag{5}$$

where t is the time of arrival of the signal, $\beta^2 = m/2kT$, k is Boltzmann constant.

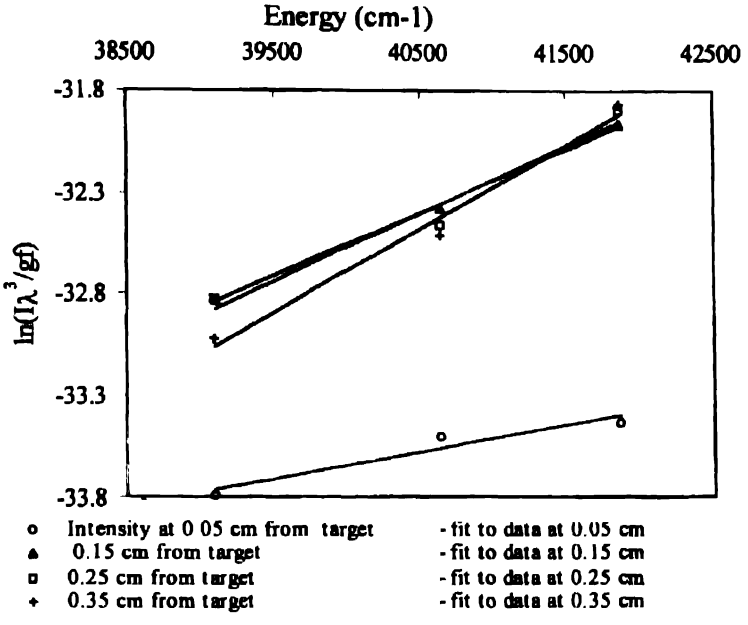

Figure 8. Boltzmann plots of data

Kools *et al* [14] have described the plume expansion on hydrodynamic model. The laser pulse is assumed to generate an elliptical gas cloud from the solid. The gas cloud equillibriates to a full MB distribution in the C.O.M. system. Zheng *et al.* [15] have tried to fit the TOF distribution on the isentropic supersonic expansion model. Signal at different times is given as

$$\text{signal} = B\left(\frac{d}{t}\right)^3 \exp\left(-\beta^2\left(\frac{d}{t} - V_0\right)^2\right) \tag{6}$$

where A and B of equations (4) and (6) are constants adjusted to make peak signal coincide with calculated values. At the distance of 0.5 mm from the target experimentally measured TOF distribution after subtracting the continuum background is given in Figure 9. The signal height on the TOF trace denotes the number of particles of particular species, in this case the atoms emitting 4104.7 Å line, arriving between t and $t + dt$. Eq. (4) fits the experimental curve if emission at two different temperatures are superposed. Theoretical fitting to the experimental measurement is shown in Figure 9.

3.4 Linewidth measurements :

Near the target spectral lines are observed with very large width and shift (Figures 10 and 11). In this region there is continuum background. However the continuum decays faster than the

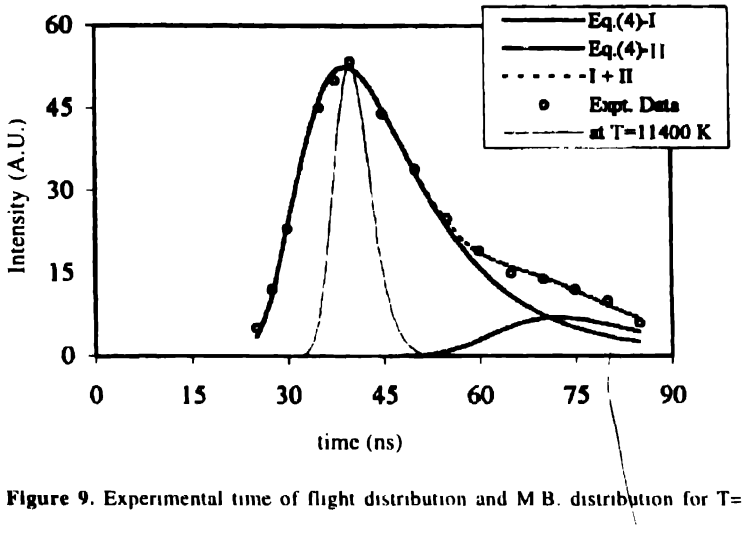

Figure 9. Experimental time of flight distribution and M B. distribution for T=11400K

line. The fluorescence line shape is affected by Stark broadening resulting from Coulomb interaction of the emitting species. Stark broadening is explained on impact broadening theory where the interaction between emitters and electrons is considered as collision. Choice of the line is made according to following conditions : (a) Stark broadening is very large for the transition such that other broadenings can be neglected ; (b) line is not overlapped by other lines ; (c) for the line self absorption is negligible. Line broadening is maximum at 0.5 mm from the target and decreases as the plume propagates away from the target. At 3.5 mm and beyond it has constant value equal to the instrumental width. At 0.5 mm the width evolves in space as

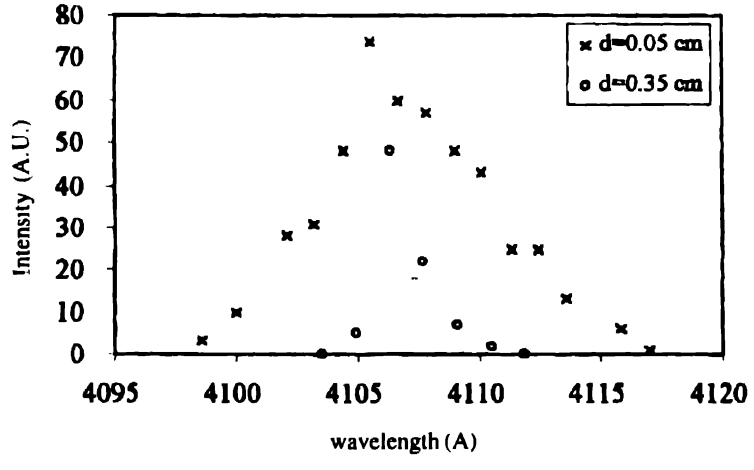

Figure 10. Line profile of 410.47 nm at 0.5 mm and 3.5 mm from the target

well as in time as shown in the Figures 12 and 13. It is observed that width is maximum between 35 to 40 ns. Background continuum in the neighbourhood of the lines decays in 30 ns. Width measurements are carried out at signal averager aperture delay of 40 ns. There was no sign of

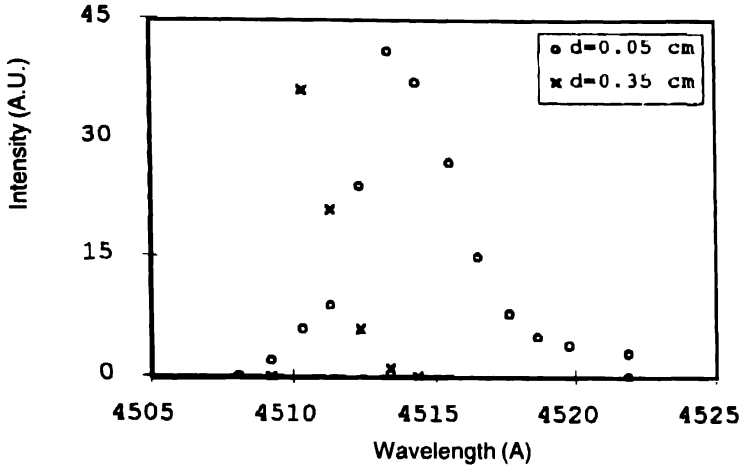

Figure 11. Line profile of 451.13 nm at 0.5 mm and 3.5 mm from the target.

self absorption. At the distance of 0.5 mm from the target the motion is only in the forward direction and the Doppler width is negligible in the transverse direction in which measurements are made. Natural width is 1.21×10^{-4} Å. At 3.5 mm width recorded is taken as instrumental

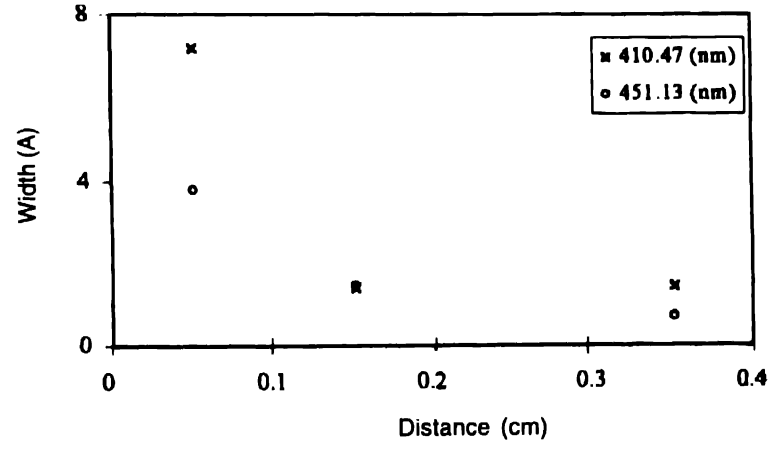

Figure 12. Space evolution of width

width due to monochromator and recording instrument. The experimentally measured width is scaled accordingly and after subtracting the instrumental width the values are used to calculate number density N. Experimentally recorded widths are given in table 2. The lines at 0.5 mm are also shifted. On impact approximation width and shift are given by Griem [16]. Experimentally observed width at the measured temperature of 11400 K corresponds to electron number density $N = 6 \times 10^{17}$ cm^{-3} for 4104.7 Å line and $N = 5 \times 10^{17}$ cm^{-3} for 4511.3 Å line.

Table 2. Observed widths

Line (Å)	Distance (mm)	FWHM (width (Å)
4104.7	0 5	7 2
	1 5	1.4
	3 5	1.4
4511 3	0 5	3 8
	1 5	1 5
	3 5	0 7

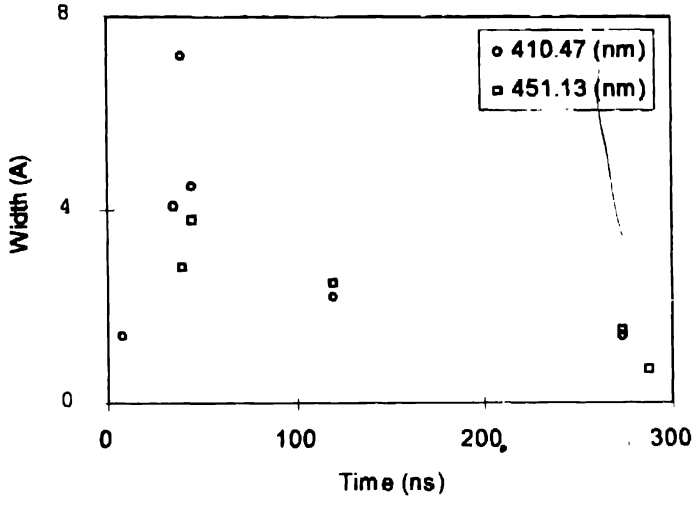

Figure 13. Time evolution of width

4. Discussion

From the plume propagation studies, it is concluded that the drag model holds good near the target. This conclusion is supported by the following facts (i) departure of eq. (2) from the experimental values is between 30-40% in this region whereas experimental error is 7%. (ii) The drag model fit is within experimental error limits for different ambient gases. (iii) We have studied for other solid targets *viz.*, Cu, Cd, Zn, Sn and Mn where the eq. (2) fails to reproduce the experimental values but the drag model holds good close to the target.

Stopping distance Vp/C is 4.9 cm, 2 cm and 1.95 cm for 1 torr He, Ar and air respectively. It is found to decrease as the atomic weight of the ambient gas. In air it is less than in Argon. Likely cause of this is the difference in their reactivity. Beyond 2.5 mm, eq. 2 holds good. Power of t is 0.6 for Argon which corresponds to plane shock formation. For Helium and air at 0.1 torr it is 0.89 and 1. In air at 1 Torr n is 0.8. When mass of the shocked gas is small compared to the mass of the ejecta linear dependence of distance with time is predicted [11]. For light atoms or low pressure of ambient gas the propagation is tending to free expansion.

Emission of 4104.7 Å line is from the low lying excited state $5s^2 6s\ ^2S$. It has life time of 7.4 ns. [17] The intensity of the line is maximum at 1.5 mm from the target whereas the temperature and line width have maximum at 0.5 mm from the target. Atoms reach 1.5 mm after 70 ns from the time of leaving the target. This shows that the $5s^2 6s\ ^2S$ state atoms are produced before ejection and also after in other mechanisms like : (i) ion electron recombination ; (ii) collisions of ground state ; (iii) stepwise emission from higher states. Target evaporates when the short laser pulse is incident on it. The evaporation may continue beyond the pulse duration. The vapour consists of ions, electrons and neutral atoms. When nanosecond laser pulses cause sputtering of target surfaces gas phase interactions of the material cause Knudsen layer which evolves into unsteady adiabatic expansion (UAE) [18] for which the particle motion is characterized by forward peaking and high Mach number. Spatial evolution is proportional to time in UAE. KL thickness [19] for Indium was calculated under experimental conditions and was found to be in microns which is much smaller than the distance where TOF is measured. The plasma front moves with velocity

$$u = u_k \cdot (1 + \gamma)/(1 - \gamma),$$

Where u_k is velocity at KL boundary and it is also equal to sound velocity in the reservoir from which particles come out. If particles are monoatomic $\gamma = 5/3$ and $u = 3.5$ times sound velocity. If the material ejected includes ions and excited atoms γ will be between 1.2 to 1.3 [19] and u will be 7 to 10 times sound velocity. Sound velocity is $(\gamma kT/m)^{0.5}$. For Indium at 0.5 mm, sound velocity is 1.17×10^5 and 1.04×10^5 for $\gamma = 1.667$ and 1.3 respectively. Velocity estimated from the time of arrival of the signal is 1.25×10^6 cm/s which is 11 or 12 times velocity of sound. Kelly [18] has derived the expression for ablation in vacuum. In the present investigation pressure in the plasma chamber is 100 m Torr air. Puretzky *et al* have observed front edge propagation velocity 1.4×10^6 cm/s in KrF laser produced plasma on graphite target [20].

The TOF distribution for 11400 K is shown in Figure 9. Experimental TOF distribution has a tail at later times. With a single distribution with very high temperature experimental curve could not be reproduced. Experimental curve is broad and superposition of two distributions corresponding to $T_1 = 1.59 \times 10^5$ K and $T_2 = 1.72 \times 10^4$ K are required to fit the experimental curve. Vanveen *et al* [21] have also observed that the main peak is followed by a second peak. The value 1.59×10^5 is rather high. It corresponds to K.E. of 13.7 eV whereas laser photon energy is 3.68 eV. Multiphoton absorption has been shown to be the initial step in metal ablation by Mathias *et al* [22]. Energy absorbed in multiphoton process by atoms may be transferred to the surface so that the atoms are thrown off with large kinetic energy. Abnormal temperatures and forward peaking of velocity is expected if the emission process is photochemical in nature [18]. Similar experimental obsevations are expected in KL formation also. For Cu target temperature 3×10^4 K has been reported by Herden and Bloss [4] in N_2 laser produced plasma and 2.3×10^4 K by Peitsch [23] in XeCl laser produced plasma.

Appreciable Stark width is observed upto 60 ns at 0.5 mm. Intensity of 4104.7 Å line is maximum around 60 ns at 0.5 mm and then it drops. The major contribution to the upper state population is likely to be recombination of ions and electrons after they leave the target. Because of the large expansion velocity ($\sim 10^6$ cm/s), the density of particles and intensity of spectral line drop beyond 60 ns.

5. Conclusions

(i) There is KL formation near the target.

(ii) The luminous front moves proportional to time in He and Air at 1 torr and Air at 100 mtorr but there is plane shock formation in Ar at 1 torr.

(iii) There is large excitation temperature gradient between 0.5 – 1 mm.

(iv) The time of flight distribution of neutral atoms is very broad.

Acknowledgments

One of the authors (SVI) is grateful to the Department of Science and Technology, Government of India for financial assistance in the form of research project.

References

[1] K Kagawa and S Yokoi *Spectrochem Acta* **37B** 9 (1982)

[2] Sharada Itagi, V V Itagi, S S Patil, A R Khan and A J Pathan *Indian J Pure Appl Phys* **28** 44 (1990)

[3] A G Bidve, Sharada Itagi, P S Kulkarni and A J Pathan *Indian J Pure Appl Phys* **35** 241 (1997)

[4] W Herden and W H Bloss *Appl Phys Lett* **31** 2 (1977)

[5] K Kagawa, S Yokoi and S Nakajima *Optics Commun* **45** 4 (1983)

[6] K Kagawa, N Othani, S Yokoi and S Nakajima *Spectrochem Acta* **39B** 4 (1984)

[7] A Namiki, T Kawai and K Ichige *Surf Sci* **166** 129 (1986)

[8] J F Ready *Industrial Applications of Lasers* (New York · Academic) (1978)

[9] D B Geohegan *Appl Phys Lett* **60** 22 (1992)

[10] J Gonzalo, F Vega and C N Afonso *J Appl Phys* **77** 12 (1995)

[11] A Gupta, B Baren, K G Casey, B W Hussey and R Kelly *Appl Phys. Lett.* **59** 11 (1991)

[12] C H Corliss and W R Bozman *Experimental transition probabilities for spectral lines of seventy elements (National Bureau of Standard Monograph 53)* (Washington DC U S Government Printing Press) (1962)

[13] R Kelly and R W Dreyfus *Surf Sci.* **198** 263 (1988)

[14] J G S Kools, T B Baller, S T Dezwart and J Dieleman *J Appl Phys* **71** 9 (1992)

[15] J P Zheng, Q Huang, D T Shaw and H S Kwok *Appl Phys Lett* **54** 3 (1989)

[16] H S Griem *Plasma Spectroscopy* (New York Mc Graw-Hill) (1964)

[17] C E Moore *Atomic Energy Levels (Circular of National Bureau of Standards 467)* (Washington DC . U S Govt Printing Press) (1958)

[18] R Kelly *J Chem Phys* **92** 8 (1990)

[19] J Hermann, A I Thomann, C Boulmer-Leborgnu, B Dubreuil, M L De Giorgi, A Perrone, A Luches and I N Mihailescu *J Appl Phys.* **77** 7 (1995)

[20] A A Puretzky, D B Geohegan, R E Haufler, R L Hettich, X Y Zheng and R N Compton *Laser Ablation · Mechanisms and Applications (II AIP Conference Proceedings 288)* eds J C Miller and D B Geohegan (1994)

[21] G N A Vanveen, T Baller and A E De Vries *J. Appl Phys.* **60** 10 (1980)

[22] E Mathias, S Petzoldt, A P Elg, P J West and J Reif *Laser induced Damage in Optical Materials* (NBS spetial publication) (1987)

[23] W Pietsch *J Appl Phys* **79** 3 (1996)